

Anthranilic Acid Amides: A Novel Class of Antiangiogenic VEGF Receptor Kinase Inhibitors

Paul W. Manley,* Pascal Furet, Guido Bold, Josef Brügggen, Jürgen Mestan, Thomas Meyer, Christian R. Schnell, and Jeanette Wood

Oncology Research, Novartis Pharma AG, CH-4057 Basel, Switzerland

Martin Haberey, Andreas Huth, Martin Krüger, Andreas Menrad, Eckhard Ottow, Dieter Seidelmann, Gerhard Siemeister, and Karl-Heinz Thierauch

Schering AG, Research Laboratories, D-13342, Berlin, Germany

Received April 4, 2002

Two readily synthesized anthranilamide, VEGF receptor tyrosine kinase inhibitors have been prepared and evaluated as angiogenesis inhibitors. 2-[(4-Pyridyl)methyl]amino-*N*-[3-(trifluoromethyl)phenyl]benzamide (**5**) and *N*-3-isoquinolyl-2-[(4-pyridylmethyl)amino]benzamide (**7**) potently and selectively inhibit recombinant VEGFR-2 and VEGFR-3 kinases. As a consequence of their physicochemical properties, these anthranilamides readily penetrate cells and are absorbed following once daily oral administration to mice. Both **5** and **7** potently inhibit VEGF-induced angiogenesis in an implant model, with ED₅₀ values of 7 mg/kg. In a mouse orthotopic model of melanoma, **5** and **7** potently inhibited both the growth of the primary tumor as well as the formation of spontaneous peripheral metastases. The anthranilamides **5** and **7** represent a new structural class of VEGFR kinase inhibitors, which possess potent antiangiogenic and antitumor properties.

Introduction

Angiogenesis is a multistep process, whereby new capillaries sprout and grow from existing blood vessels. This process is tightly regulated and only occurs in normal adult tissues during the female reproductive cycle and tissue repair. In cancer, angiogenesis is crucial for supplying growing tumors with a vasculature to provide nutrients and remove waste products, as well as providing a conduit for the dispersal of metastases.^{1,2} A key pro-angiogenic cytokine released by many tumor types is vascular endothelial growth factor (VEGF). The angiogenic activity of the VEGF family of proteins is mediated by two high affinity receptors, VEGFR-1 and VEGFR-2 located on vascular endothelial cells, with a third, VEGFR-3 which mediates lymphangiogenesis, found on lymphatic vessels.^{3–5} These VEGFR receptors are members of the receptor tyrosine kinase family and comprise an extracellular ligand binding domain, a transmembrane domain, and an intracellular, split kinase domain. VEGF is a heterodimeric protein, which binds to two adjacent VEGF receptors, causing them to dimerize, whereupon the tyrosine kinase domains become activated, bind ATP, and catalyze the transfer of the γ -phosphate from the ATP-Mg²⁺ complex to the hydroxy group of a tyrosine residue. These cytosolic phosphorylated sites can then serve as binding sites for other substrates, which in turn may be phosphorylated as part of a signal transduction cascade. Because of the tissue localization of the receptors and the tight control of angiogenesis, VEGFR-kinase inhibition presents an

attractive approach to selectively inhibit tumor growth and metastasis, without affecting the surrounding normal tissue.

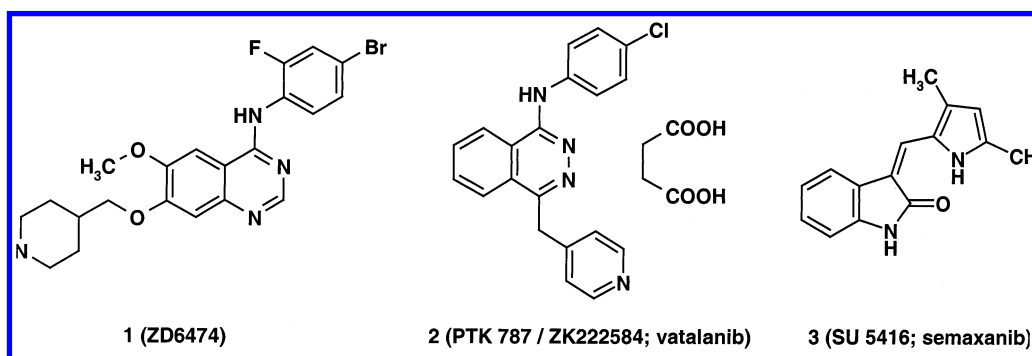
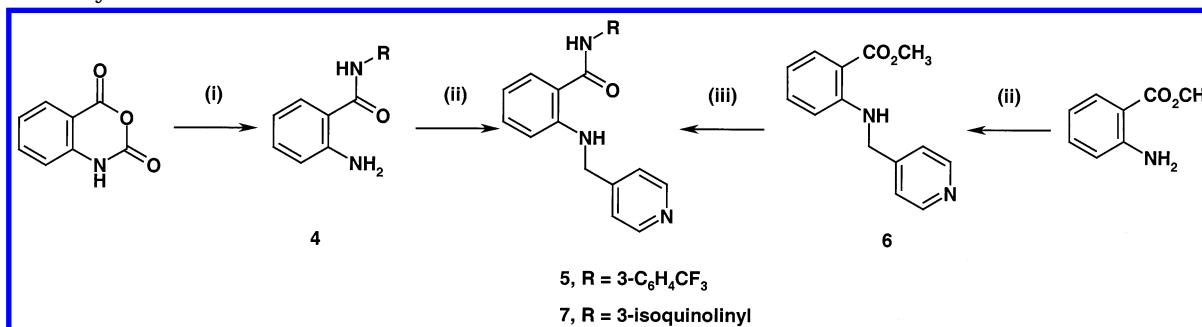
Because of the difficulties associated with the competitive inhibition of protein–protein interactions by small molecular weight compounds,⁶ modulating the activity of kinases by interfering either with ligand or substrate binding is difficult and targeting the catalytic site of kinases with ATP-competitive inhibitors is a more promising approach for drug intervention.⁷ To this end, there are several VEGFR kinase inhibitors (**1–3**) currently undergoing clinical evaluation in cancer patients, belonging, respectively, to either the quinazoline,^{8,9} phthalazine,^{10–12} or indolinone¹³ chemical classes (Chart 1). In this communication, we describe two new compounds, **5** and **7**, structurally elaborated from an anthranilamide scaffold.

Chemistry. The anthranilamides may be conveniently prepared in two steps (Scheme 1). Thus, ring opening of isatoic anhydride with 3-trifluoromethylaniline affords the amine **4**, which upon reductive alkylation with 4-pyridinecarboxaldehyde affords the anthranilamide, **5**. In an alternative synthesis, reductive alkylation of methyl anthranilate affords the amine **6**, which is then subjected to Weinreb amidation,¹⁴ to give the anthranilamide **7**.

Compounds **5** and **7** are stable crystalline solids. Although they have relatively low aqueous solubilities (2 μ g/mL) at pH 6.8 in phosphate buffer, as a consequence of the basicity of both compound **5** (p*K*_a 5.2) and compound **7** (p*K*_a 5.1, 2.7),¹⁵ their solubilities markedly increase with decreasing pH (solubility at pH 1.0 > 200 μ g/mL). Furthermore, the topological polar surface areas of the compounds (TPSA 45.0 and 52.8 Å² for **5** and **7**,

* To whom correspondence should be addressed. Tel: 0041 61 6966878. Fax: 0041 61 6966246. E-mail: paul.manley@pharma.novartis.com.

Chart 1

Scheme 1. Synthesis of Anthranilamides^a

^a Reagents: (i) 3-trifluoromethylaniline, DMF, 100 °C; (ii) 4-pyridinecarboxaldehyde, NaCNBH₃, AcOH, MeOH; (iii) 3-isoquinolineamine, AlMe₃, toluene.

Table 1. Comparative Activities of the Anthranilamides **5** and **7**, the Phthalazine PTK787 and the Quinazoline ZD6474 against the VEGF Receptor Kinases and a Selection of Other Tyrosine Kinases^{a-c}

KINASE ^b	5	7	ZD6474	PTK787	SU5416
VEGFR-1 (Flt-1)	130 ± 81; <i>n</i> = 5	130 ± 30; <i>n</i> = 3	90 ± 10; <i>n</i> = 7 (1600 ± 400) ^c	110 ± 25; <i>n</i> = 17	43 ± 11
VEGFR-2 (human KDR)	23 ± 6; <i>n</i> = 9	9 ± 1; <i>n</i> = 4	17 ± 3; <i>n</i> = 5 (40 ± 10) ^c	42 ± 3; <i>n</i> = 37	220 ± 34 (1300 ± 800) ^d
VEGFR-3 (Flt-4)	18 ± 1; <i>n</i> = 2	52 ± 1; <i>n</i> = 3	233 ± 52; <i>n</i> = 6	195 ± 30; <i>n</i> = 6	50
PDGFR-β	640 ± 100; <i>n</i> = 4	357 ± 130; <i>n</i> = 3	477 ± 84; <i>n</i> = 4 (1100 ± 300) ^c	490 ± 52; <i>n</i> = 14	2220 ± 1500 (37 900 ± 8900) ^d
c-Kit	236 ± 60; <i>n</i> = 4	105 ± 40; <i>n</i> = 3	343 ± 76; <i>n</i> = 4	620 ± 56; <i>n</i> = 21	660 ± 165 (35 ± 5) ^d
CSF-1R (c-Fms)	380 ± 140; <i>n</i> = 3	99 ± 21; <i>n</i> = 3	1600 ± 170; <i>n</i> = 3	1240 ± 180; <i>n</i> = 7	84 ± 4
EGFR (HER-1, ErbB)	10 400 ± 690; <i>n</i> = 4	> 10 000; <i>n</i> = 3	16 ± 3; <i>n</i> = 5 (500 ± 100) ^c	> 10 000; <i>n</i> = 4	> 10 000; <i>n</i> = 4
FGFR-1	> 10 000; <i>n</i> = 4	5100 ± 1660; <i>n</i> = 4	2310 ± 600; <i>n</i> = 4 (3600 ± 900) ^c	> 10 000; <i>n</i> = 4	> 10 000; <i>n</i> = 4 (4200 ± 800) ^d
CDK-1	> 10 000; <i>n</i> = 3	> 10 000; <i>n</i> = 3	> 10 000	> 10 000; <i>n</i> = 3	> 10 000; <i>n</i> = 3
Tie-2 (Tek)	> 10 000; <i>n</i> = 3	6800 ± 2,180; <i>n</i> = 3	567 ± 27; <i>n</i> = 6 (2500 ± 1200) ^c	> 10 000; <i>n</i> = 4	> 10 000; <i>n</i> = 3
c-Met	> 10 000; <i>n</i> = 3	> 10 000; <i>n</i> = 3	3370 ± 320; <i>n</i> = 4	> 10 000; <i>n</i> = 4	> 10 000; <i>n</i> = 3
IGF-1R	> 10 000; <i>n</i> = 3	6400 ± 200; <i>n</i> = 3	> 10 000; <i>n</i> = 3	> 10 000; <i>n</i> = 3	> 10 000; <i>n</i> = 2
c-Src	> 10 000; <i>n</i> = 3	> 10 000; <i>n</i> = 2	186 ± 19; <i>n</i> = 7	> 10 000; <i>n</i> = 4	> 10 000; <i>n</i> = 2
c-Abl	2820; <i>n</i> = 1	5330 ± 70; <i>n</i> = 3	86 ± 21; <i>n</i> = 5	> 10 000; <i>n</i> = 4	> 10 000; <i>n</i> = 1

^a Data represent the mean ± SEM (*n* determinations) drug concentrations required to inhibit enzyme activity by 50% (IC₅₀ value; nM) at the following ATP concentrations 1.0 μM (PDGFR-β, c-Kit, CSF-1R, c-Met), 2.0 μM (HER-1), 5.0 μM (c-Abl), 7.5 μM (CDK-1), 8.0 μM (VEGFR-1, VEGFR-2, FGFR-1, Tie-2), 13.0 μM (VEGFR-3), 20.0 μM (c-Src), 30.0 μM (IGF-1R), and, unless otherwise indicated are data from Novartis Pharma AG. ^b Alternative nomenclature for these kinases is given in parentheses script. ^c Published data from refs 8 and 9. ^d Published data from ref 13.

respectively),¹⁶ together with their high permeabilities (passive diffusion) across Caco-2 cell monolayers (intrinsic permeability, *P*_m = 45.2 and 21.7 × 10⁻⁵ cm/min for **5** and **7**, respectively), are predictive of intestinal absorption following oral administration.

Pharmacology. The *in vitro* potency and selectivity profiles of the compounds as kinase inhibitors were evaluated using recombinant GST-fused kinase domains

expressed in baculovirus. Assays were performed under conditions as previously described,¹⁰ with ATP concentrations similar to the *K*_m of the respective enzyme toward ATP (see legend for Table 1). IC₅₀ values were calculated by linear regression analysis of the percentage inhibition of each compound and are shown in Table 1, expressed as mean ± SEM with *n* representing the number of determinations.

Table 2. Comparative Effects of the Anthranilamides **5** and **7**, the Phthalazine PTK787, the Indolinone SU5416, and the Quinazoline ZD6474 on VEGF-induced Phosphorylation of VEGFR-2 in CHO Cells^a

compound	inhibition of VEGFR-2 autophosphorylation (IC ₅₀ ; nM)
5	1.24 ± 0.19 (<i>n</i> = 9)
7	1.16 ± 0.12 (<i>n</i> = 7)
1 (ZD6474)	2673 ± 174 (<i>n</i> = 6)
2 (PTK787)	16.0 ± 1.1 (<i>n</i> = 127)
3 (SU5416)	884 ± 46 (<i>n</i> = 12)

^a Results are given as IC₅₀ values, expressed as mean ± SEM, *n* = number of experiments.

Table 3. Pharmacokinetic Parameters of Compounds **5** and **7**, Following Single Oral Administration to Female MAG Mice (50 mg/kg)^a

compound	plasma C _{0.5h} (μmol/L)	plasma C _{1.0} (μmol/L)	plasma C _{1.5h} (μmol/L)	plasma C _{2h} (μmol/L)
5	9.5 ± 2.1	4.7 ± 2.1	1.5 ± 0.8	1.1 ± 0.3 ^b
7	3.4 ± 0.1	1.9 ± 0.4	1.9 ± 0.4	1.6 ± 0.2 ^c

^a Both **5** and **7** were formulated in 5% DMSO/0.5% TWEEN 80. At allotted times mice were sacrificed, blood removed, and the concentration of drug in the plasma was determined by reverse-phase HPLC. Data are expressed as mean ± SEM, *n* = 4.

^b Following once-daily dosing for 20 days, the C_{2h} value for **5** was 1.75 ± 0.23. ^c At an additional time point after 3 h, the plasma C_{3h} value for **7** was 1.3 ± 0.4.

Since a VEGFR-kinase inhibitor must enter cells to bind to the kinase domain of the receptor, the effects of the compounds were tested in a cellular assay, using Chinese hamster ovary (CHO) cells transfected with human VEGFR-2.¹¹ Autophosphorylation of the VEGFR-2 receptor kinase was induced with VEGF. After lysis of the cells, the degree of phosphorylation was measured by capture of the VEGFR-2 with a specific monoclonal antibody, followed by quantification of receptor phosphorylation with an anti-phosphotyrosine antibody using a chemiluminescent assay. The influence of the compounds on autophosphorylation was calculated as percentage inhibition and dose–response curves were used to calculate IC₅₀ values, which are presented in Table 2 and expressed as mean ± SEM with *n* representing the number of experiments.

Prior to evaluating their effects in vivo, the compounds were first tested to ascertain whether they were absorbed following oral administration. Plasma concentrations of drug substance were determined by HPLC/UV in normal mice after a single oral dose of 50 mg/kg, dissolved in a mixture of 5% DMSO and 0.5% Tween 80 in water, and administered by gavage. The pharmacokinetic parameters derived from these data are summarized in Table 3.

The capacity of the compounds to modulate angiogenesis in animals was assessed in a growth factor implant model.¹¹ In immunocompetent mice, both VEGF and basic fibroblast growth factor (bFGF) induce the growth of vascularized tissue around subcutaneous implants which contain either of these growth factors. The response is concentration-dependent and can be quantified by measuring the haemoglobin (blood) content of the tissue. The response can be specifically blocked by selective inhibitors of these growth factors and their signaling pathways. The antiangiogenic activity of the drug substances in this model were compared

at a standard oral dose of 50 mg/kg, with the exception of SU5416 which was administered at 50 mg/kg intraperitoneally. For the anthranilamides **5** and **7**, the dose dependency of the response was evaluated, with ED₅₀ values being calculated from the dose–response curves (Figure 1).

The effects of the compounds on tumor growth and metastasis was evaluated in a mouse orthotopic model of melanoma.¹⁷ Intradermal injection of B16/BL6 melanoma cells into the ears of immunocompetent C57BL/6 mice leads to the formation of a primary tumor and metastases in the regional lymph nodes. The size of the primary tumor can be quantified microscopically, with a computerized imaging system. The effect of drug substances on the formation of metastases is quantified by the weight of surgically removed cervical lymph nodes.

Results and Discussion

The anthranilamides are highly potent and selective inhibitors of the recombinant VEGFR-2 and VEGFR-3 kinases, with compound **5** possessing IC₅₀ values of 23 and 18 nM and compound **7** of 9 and 52 nM, respectively. At 3- to 5-fold higher concentrations, they also inhibit VEGFR-1 and, although they possess some activity against other members of the PDGFR kinase family at submicromolar concentrations (cKit, CSF-1R, and PDGFR-β), they do not significantly inhibit any of the other kinases tested at concentrations <10 μM (Table 1). The aniline **4** and the ester **6** were devoid of activity (data not shown). In this respect, compounds **5** and **7** possess a comparable selectivity profile in comparison to clinical development compounds such as PTK787/ZK222584, SU5416, and ZD6474 (Table 1).

Both anthranilamides are capable of penetrating cells and inhibit the VEGF-stimulated tyrosine autophosphorylation of human VEGFR-2 in CHO cells (Table 2). The potency of compounds **5** and **7** together with that of PTK787 (**2**) in this assay parallels that found for the inhibition of recombinant VEGFR-2 transphosphorylation. However, a large discrepancy exists for ZD6474 and SU5416 between the two assays. The reason for this lack of concordance is not clear, particularly since both compounds have been reported to inhibit the VEGF-induced proliferation of human umbilical vein endothelial cells.^{8,9,13}

Following oral administration to mice, both **5** and **7** were absorbed (Table 3), with plasma levels after 2 h being 880-fold and 1100-fold, respectively, greater than the corresponding IC₅₀ values for the inhibition of cellular VEGFR-2 autophosphorylation. In addition, once-daily dosing of **5** (50 mg/kg po) for 20 days had no effect on the C_{2h} value, indicating that the pharmacokinetic parameters, at least for this compound, remain stable following chronic dosing. Consequently, oral administration of 50 mg/kg of either compound would be expected to inhibit in vivo responses mediated by VEGFR-2 kinase activity, in a fashion similar to that demonstrated for other VEGFR-2 kinase inhibitors.^{8,11,13} Consistent with their in vitro profiles for the inhibition of tyrosine kinases, coupled with their ability to penetrate cells to inhibit their target enzymes and their oral bioavailability in mice, in the implant model, at the standard oral dose of 50 mg/kg, compounds **5** and **7**

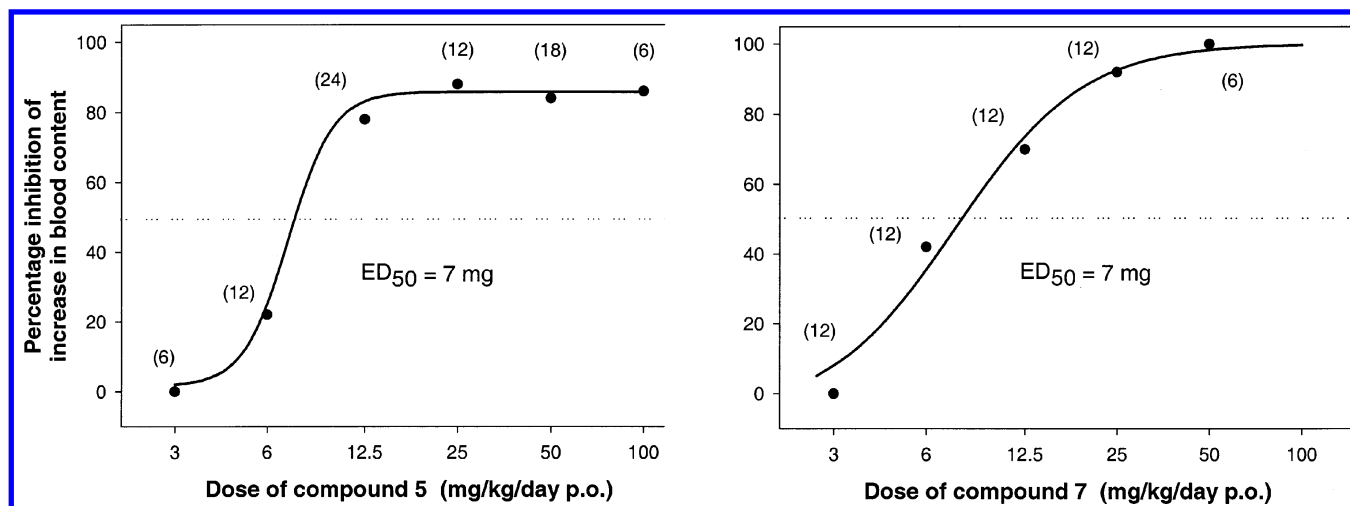


Figure 1. Anti-angiogenic activity of compounds **5** and **7** in a growth factor-stimulated implant model in mice. Results of multiple independent experiments ($n = 6$ animals per group) are expressed as percent inhibition of the growth factor-induced increase in blood content of the tissue growing around the implanted chamber. ED₅₀ values were estimated from the dose–response curve. The number of animals per dose is indicated in parentheses alongside each data point.

Table 4. Effects of Compounds on VEGF- and bFGF-induced Response in a Growth Factor Implant Model and on Primary Tumor Growth and Formation of Lymph Node Metastasis in a B16 Melanoma Model

compound	mean percent inhibition of response at 50 mg/kg po			
	growth factor-induced angiogenesis		B16 melanoma xenograft model	
	VEGF	bFGF	primary tumor growth	lymph node metastasis
5	84	77	44	85
7	100	61	39	73
PTK787	68	66	34	55
SU5416	65 ^b	87 ^b	<i>n.d.</i> ^c	<i>n.d.</i>
ZD6474	71	47	60	61

^a Results are expressed as the mean percent inhibition of ≥ 12 animals. ^b Data obtained with an intraperitoneal dose of 100 mg/kg. ^c *n.d.* = not determined.

inhibited the VEGF-induced increase in tissue blood content by 84% and 100%, respectively (Table 4). In comparison, PTK787/ZK222584, SU5416 (tested by the intraperitoneal route),¹⁸ and ZD6474 also showed activity, although with significantly less efficacy. To further characterize the efficacy of the anthranilamides against VEGF mediated angiogenesis, the dose–response relationships of the compounds were investigated: Both compounds **5** and **7** dose-dependently inhibited angiogenesis induced by VEGF with an ED₅₀ value of 7 mg/kg (Figure 1). The efficacy of compound **7** was slightly greater than that of **5**. Surprisingly, despite being devoid of significant activity against the FGFR-kinase (Table 1), the compounds in this study showed efficacy at inhibiting bFGF-induced angiogenesis, with **5** for example inhibiting bFGF-induced angiogenesis to the extent of 77% at 50 mg/kg po (ED₅₀ 5 mg/kg). We have reported similar findings with other selective VEGFR-2 kinase inhibitors and taken together these suggest that in vivo responses to bFGF in this model might be mediated by the endogenous VEGF/VEGFR system.^{19,20}

The B16/BL6 mouse melanoma is an established cancer model, in which both a primary tumor and spontaneous metastases are formed in the cervical lymph nodes and in the lungs.¹⁷ It has been demonstrated that both the primary tumor and the metastases

produce VEGF and bFGF (protein by ELISA and mRNA by real-time PCR) and it has also been shown that several human melanoma cell lines also express VEGF.^{21,22} In this model, both compounds **5** and **7** inhibited primary tumor growth as well as the formation of metastases and there were no deaths or overt signs of toxicity in any drug treatment group. Oral administration of **5**, from day 7–21 following tumor cell injection, dose dependently inhibited primary tumor growth (Figure 2, upper left) with an ED₅₀ value of 50 mg/kg and the formation of lymph node metastases (Figure 2, lower left) with an ED₅₀ value less than 25 mg/kg. Effects in animals receiving once-a-day dosing were similar to those in which the dose was split and administered twice-a-day (data not shown). Compound **7** showed similar efficacy to **5** in these models, although there was an indication that twice-daily dosing is more efficacious both against orthotopic tumor growth and the formation of lymph node metastases (data not shown). The observation that the development of lymph node metastases was inhibited to a greater extent than was the growth of the primary tumor may reflect an additional direct antimetastatic effect of the compounds. The phthalazine, PTK787, and the quinazoline, ZD6474, also showed efficacy in this melanoma model, with ZD6474 in comparison with the other compounds, appearing to be more effective against primary tumor growth (Table 4). This observation might be a result of ZD6474 having an advantageous pharmacodynamic profile or possessing an additional mechanism of action affecting primary tumor growth.

Conclusion

The anthranilamides **5** and **7** are highly potent and selective inhibitors of recombinant VEGFR-kinase, which readily penetrate cells to inhibit VEGFR-2 autophosphorylation. As a consequence of their physicochemical properties and their cell permeability, the anthranilamides are orally absorbed following administration to mice. In keeping with these properties, the compounds potentially inhibit angiogenesis with high efficacy in an implant model in immunocompetent mice. Furthermore, in an orthotopic melanoma model, the antiangiogenic

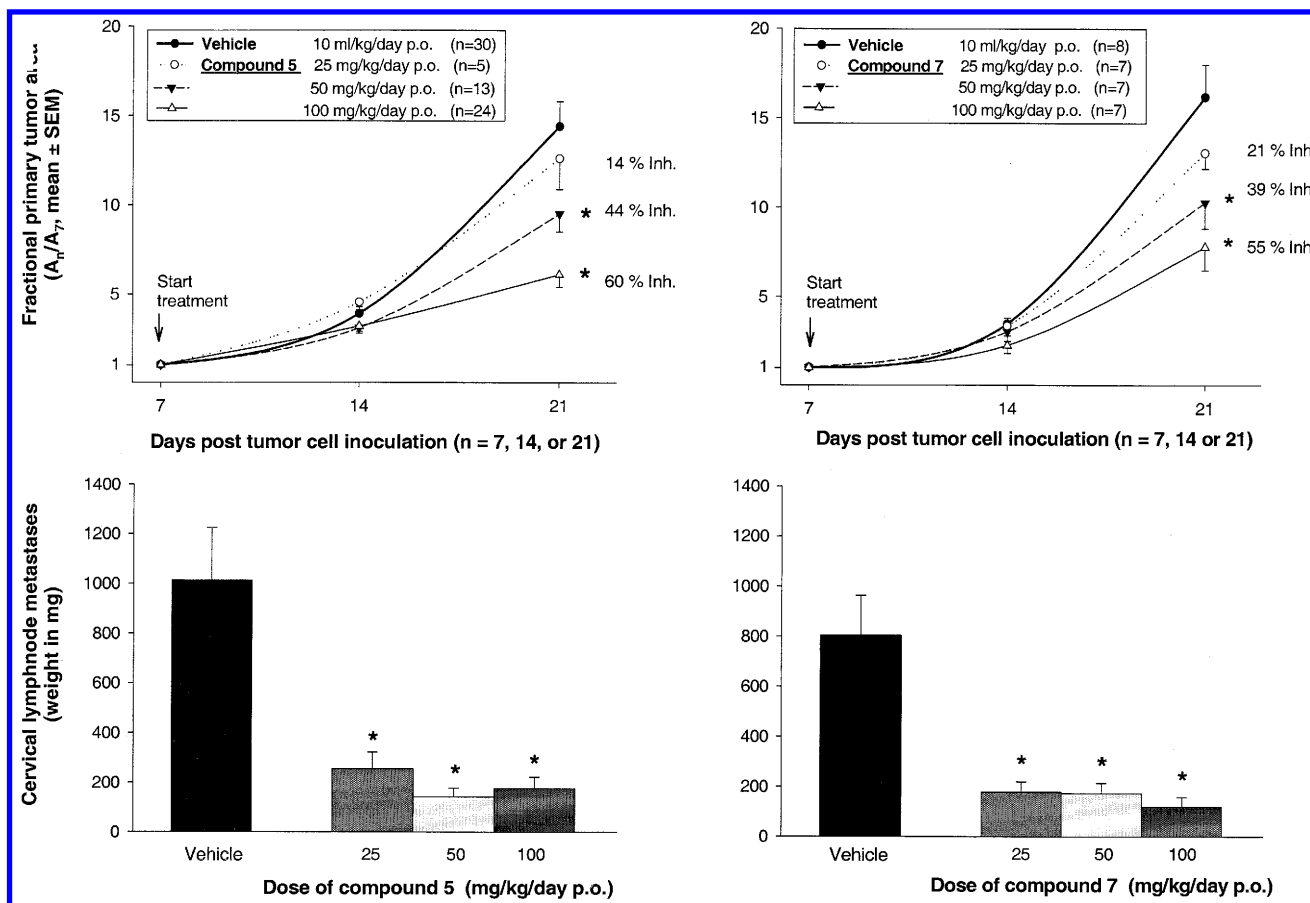


Figure 2. Dose-dependent antitumor and antimetastatic effects of compounds **5** (left) and **7** (right) in a B16/BL6 melanoma orthotopic model in C56BL/6 mice after oral administration. Dose-response effects on primary tumor growth are expressed in terms of relative mean tumor area quantified on day 14 (A_{14}) and day 21 (A_{21}) after intradermal injection into the ears, compared to that on day 7 (A_7), and are shown in the upper panels; percent inhibition on day 21 (14 days treatment) is given for each curve. Absolute tumor mean areas at day 7 (A_7) were in the range 0.97 ± 0.09 to 1.42 ± 0.13 mm² and not statistically different. The influence of the compounds on cervical lymph node metastases, quantified by the weight of the cervical lymph nodes after surgical removal, are shown in the panels below. Values are mean \pm SEM, * $P < 0.5$, ANOVA, Dunns, significance compared to vehicle-treated group.

activity of the anthranilamides **5** and **7** translates into potent inhibition of both primary tumor growth and the formation of lymph node metastases. Upon chronic oral dosing in rodents, the compounds are well tolerated with no overt signs of toxicity. Consequently, these anthranilamides represent a new structural class of VEGFR kinase inhibitors, possessing potent antiangiogenic and antitumor properties, with comparable selectivity for VEGFR-kinases compared to other small molecular weight compounds currently undergoing clinical evaluation.

Experimental Section

Flash chromatography was performed using silica gel (E. Merck, Grade 60, particle size 0.040–0.063 mm, 230–400 mesh ASTM) with the eluent indicated. Melting points were determined on a Leitz Kofler hot-stage apparatus and are uncorrected. Proton NMR spectra were recorded at 300 K with a Bruker DRX500 instrument (500 MHz) using deuterated DMSO as internal standard. Chemical analyses, indicated by the symbols of the elements, were performed by Solvias AG (Basel) and results obtained were within $\pm 0.4\%$ of the theoretical values.

2-Amino-*N*-[3-(trifluoromethyl)phenyl]benzamide (**4**).

A mixture of 3-(trifluoromethyl)aniline (9.7 g, 60 mmol) and isatoic anhydride (9.75 g, 60 mmol) in DMF (80 mL) was stirred at 100 °C for 18 h. The solvent was evaporated off under reduced pressure to give a residue which was dissolved in

EtOAc (300 mL) and washed with saturated aqueous ammonium chloride. The solution was dried (Na_2SO_4) and filtered and the solvent was evaporated off under reduced pressure to yield the crude product which was recrystallized from EtOAc–hexane to give **4** as colorless needles (6.3 g, 37%): mp 132–133 °C; NMR ($\text{DMSO}-d_6$) δ 6.38 (sbr, 2H), 6.60 (ddd, $J = 8.0, 8.0, 0.7$ Hz, 1H), 6.77 (dd, $J = 8.2, 0.7$ Hz, 1H), 7.22 (ddd, $J = 8.0, 8.0, 1.3$ Hz, 1H), 7.43 (dm, $J = 7.7$ Hz, 1H), 7.57 (ddd, $J = 8.4, 7.9$ Hz, 1H), 7.66 (dd, $J = 8.0, 1.3$ Hz, 1H), 7.96 (dm, $J = 8.4$ Hz, 1H), 8.21 (s, 1H) and 10.28 (s, 1H). Anal. ($\text{C}_{14}\text{H}_{11}\text{F}_3\text{N}_2\text{O}$) C, H, N.

2-[(4-Pyridyl)methyl]amino-*N*-[3-(trifluoromethyl)phenyl]benzamide (5**).** A stirred solution of **4** (28.0 g, 100 mmol) and acetic acid (5 mL) in MeOH (300 mL) was treated with 4-pyridinecarboxaldehyde (11 mL, 120 mmol) and stirred at 22 °C for 7 h. Sodium cyanoborohydride (21 g of 95%, 320 mmol) was then added in portions over 1 h and the mixture was stirred for a further 17 h. The solvent was evaporated off under reduced pressure and the residue was treated with CH_2Cl_2 (500 mL) and washed with saturated aqueous NaHCO_3 (500 mL), followed by saturated aqueous NaCl (100 mL). The solution was dried (Na_2SO_4) and filtered and the solvent was evaporated off under reduced pressure to yield the crude product which was recrystallized from EtOAc–hexane to give **5** as a colorless crystalline solid (23 g, 62%): mp 158–160 °C; NMR ($\text{DMSO}-d_6$) δ 4.51 (d, $J = 6.2$ Hz, 2H), 6.55 (d, $J = 8.4$ Hz, 1H), 6.67 (ddd, $J = 7.7, 7.3$, and 0.6 Hz, 1H), 7.26 (ddd, $J = 8.3, 7.3$, and 1.2 Hz, 1H), 7.34 (dm, $J = 6.0$ Hz, 2H), 7.45 (dbr, $J = 7.9$ Hz, 1H), 7.59 (t, $J = 8.0$ Hz, 1H), 7.74 (dd, $J = 7.8$ and 1.4 Hz, 1H), 7.96 (t, $J = 6.2$ Hz, 1H), 7.98 (dbr, $J =$

8.0 Hz, 1H), 8.28 (sbr, 1H), 8.49 (dm, $J = 6.0$ Hz, 2H) and 10.47 (s, 1H). Anal. ($C_{20}H_{16}F_3N_3O$) C, H, N.

2-[(4-Pyridinylmethyl)amino]benzoic Acid, Methyl Ester (6). A mixture of methyl anthranilate (1.51 g, 10 mmol) and 4-pyridinecarboxaldehyde (1.71 g, 16 mmol) in MeOH (60 mL) was treated with AcOH (0.6 mL) and stirred at 20 °C for 18 h. Sodium cyanoborohydride (1.2 g of 95%, 17 mmol) was then added in portions over 2 h and the mixture was stirred for an additional 2 h. The solvent was evaporated off under reduced pressure and the residue was dissolved in EtOAc. The solution was washed with saturated aqueous $NaHCO_3$, followed by saturated aqueous NaCl, dried (Na_2SO_4), filtered and the solvent was evaporated off under reduced pressure. The crude product was purified by column chromatography (silica gel, 50% EtOAc in hexane) and recrystallized from 2-propanol–hexane to give **6** as a colorless crystalline solid (1.8 g, 74%): mp 85–86 °C; NMR (DMSO- d_6) δ 3.83 (s, 3H), 4.56 (d, $J = 6.1$, 2H), 6.58 (ddd, $J = 8.2$, 6.9, 1.3 Hz, 1H), 6.60 (dd, $J = 8.2$, 6.9, 1.3 Hz, 1H), 7.29 (dd, $J = 6.9$, 1.3 Hz, 1H), 7.32 (dm, $J = 5.3$ Hz, 2H), 7.82 (dd, $J = 8.2$, 1.3 Hz, 1H), 8.20 (tbr, $J = 6.1$ Hz, 1H) and 8.50 (dm, $J = 5.3$ Hz, 2H). Anal. ($C_{14}H_{14}N_2O_2$) C, H, N.

N-3-Isoquinolinyl-2-[(4-pyridinylmethyl)amino]benzamide (7). A mixture of **6** (242 mg, 1.0 mmol) and 3-isoquinolinamine (202 mg, 1.4 mmol) in toluene (3.5 mL) was treated with a solution of $AlMe_3$ in toluene (0.75 mL of 2 M, 1.5 mmol) and stirred for 1 h at 20 °C, followed by 1 h at 110 °C. The cooled mixture was treated with saturated aqueous $NaHCO_3$ and extracted with EtOAc. The combined extracts were dried (Na_2SO_4), filtered, and evaporated to yield the crude product which was recrystallized from EtOAc to give **7** as a colorless crystalline solid (237 mg, 67%): mp 134–135 °C; NMR (DMSO- d_6) δ 4.55 (d, $J = 6.4$ Hz, 2H), 6.60 (d, $J = 7.0$ Hz, 1H), 6.66 (dd, $J = 7.0$, 7.0 Hz, 1H), 7.28 (ddd, $J = 7.0$, 7.0, 1.1 Hz, 1H), 7.39 (dm, $J = 5.3$ Hz, 2H), 7.59 (dd, $J = 8.1$, 7.0 Hz, 1H), 7.76 (dd, $J = 8.1$, 7.0 Hz, 1H), 7.90 (dd, $J = 7.0$, 1.1 Hz, 1H), 7.97 (d, $J = 8.1$ Hz, 1H), 8.12 (d, $J = 8.1$ Hz, 1H), 8.18 (bdr, $J = 6.5$ Hz, 1H), 8.53 (dm, $J = 5.3$ Hz, 2H), 8.60 (s, 1H), 9.24 (s, 1H) and 10.70 (s, 1H). Anal. ($C_{22}H_{18}N_4O$) C, H, N.

Growth Factor Implant Model of Angiogenesis. Porous Teflon chambers containing VEGF (2 μ g/mL) or bFGF (0.3 μ g/mL) in 0.8% w/v agar containing heparin (20 U/mL) were implanted subcutaneously in the flank of female mice. Mice were treated orally, with the exception of SU5416 which was administered intraperitoneally, once daily with compound or vehicle (PEG 300) from 1 day before implantation of the chambers, and the animals were sacrificed for measurement of the vascularized tissues after 5 days of treatment. The chambers were recovered from the animal and the vascularized tissue formed around the implant was carefully removed. Tissue samples were treated with water (2 mL), homogenized (1 min at 24000 rpm), and centrifuged (1 h at 7000 rpm). The supernatant was filtered to avoid fat contamination and the haemoglobin content was determined spectrophotometrically at 540 nm (Drabkin method; Sigma haemoglobin #525, Sigma, Poole, U.K.). Haemoglobin measurements were converted into blood volumes using a calibration curve obtained with whole blood samples from a donor mouse. Data were quantified as the percentage inhibition of the increase in blood content with respect to that in vehicle-treated control animals (Table 4). ED_{50} values were calculated from the dose–response curve, n = number of animals at the specified dose (Figure 1). In cases where full inhibition was not achieved at doses up to 100 mg/kg, results are expressed as percentage inhibition at the highest dose tested.

Murine Melanoma Model of Tumor Growth and Metastasis. B16/BL6 cells (5×10^4 ; obtained from I. J. Fidler, Texas Medical Centre, Houston, TX), suspended in Hanks buffer containing 10% FCS, were injected intradermally into the dorsal pinna of both ears of anaesthetized syngeneic C57BL/6 mice. One week later, treatment with either drug substance or vehicle (PEG 300) was initiated. The size of the primary tumors was monitored under a light microscope,

recorded via a low-light color video camera, and quantified with a computerized imaging system (KS-400 version 3.0, Zeiss, Germany). After two weeks of daily treatment, the animals were sacrificed and the cervical lymph nodes collected and weighed. Effects on primary tumor growth are plotted as relative tumor mean area (mm^2) quantified on day 14 (A_{14}) and day 21 (A_{21}) compared to the tumor mean area (A_7) at the start of drug treatment (day 7 after tumor cell injection). Effects on cervical lymph node metastases were quantified by the relative wet weight (mg) of the collected tissue of animals treated with drug compared to that of vehicle-treated animals. Values are mean \pm SEM. * $P < 0.5$, ANOVA, Dunns, significance compared to vehicle-treated group.

References

- (1) Kerbel, R. S. Tumor angiogenesis: past, present and the near future. *Carcinogenesis* **2000**, *21*, 505–515.
- (2) McDonnell, C. O.; Hill, A. D.; McNamara, D. A.; Walsh, T. N.; Bouchier-Hayes, D. J. Tumour micrometastases: the influence of angiogenesis. *Eur. J. Surgical Oncol.* **2000**, *26*, 105–115.
- (3) Neufeld, G.; Cohen, T.; Gengrinovich, S.; Poltorak, Z. Vascular endothelial growth factor (VEGF) and its receptors. *FASEB J.* **1999**, *13*, 9–22.
- (4) Veikkola, T.; Karkkainen, M.; Claesson-Welsh, L.; Alitalo, K. Regulation of angiogenesis via vascular endothelial growth factor receptors. *Cancer Res.* **2000**, *60*, 203–212.
- (5) Makinen, T.; Jussila, L.; Veikkola, T.; Karpanen, T.; Keitunen, M. I.; Pulkkanen, K. J.; Kauppinen, R.; Jackson, D. G.; Kubo, H.; Nishikawa, S.-I.; Yla-Herttuala, S.; Alitalo, K. Inhibition of lymphangiogenesis with resulting lymphedema in transgenic mice expressing soluble VEGF receptor-3. *Nat. Med.* **2001**, *7*, 199–205.
- (6) Cochran, A. G. Antagonists of protein–protein interactions. *Chem. Biol.* **2000**, *7*, R85–R94.
- (7) Manley, P. W.; Furet, P. Prospects for Anti-Angiogenic Therapies based upon VEGF Inhibition. In *Anticancer Agents: Frontiers in Cancer Chemotherapy*; Ojima, I., Vite, G., Altmann, K., Eds.; ACS Symposium Series 796; American Chemical Society: Washington, DC, **2001**; pp 282–298.
- (8) Hennequin, L. F.; Stokes, E. S. E.; Thomas, A. P.; Johnstone, C.; Ple, P. A.; Ogilvie, D. J.; Dukes, M.; Wedge, S. R.; Kendrew, J.; Curwen, J. O. Novel 4-Anilinoquinazolines with C-7 Basic Side Chains: Design and Structure Activity Relationship of a Series of Potent, Orally Active, VEGF Receptor Tyrosine Kinase Inhibitors. *J. Med. Chem.* **2002**, *45*, 1300–1312.
- (9) Wedge, S. R.; Ogilvie, D. J.; Dukes, M.; Kendrew, J.; Chester, R.; Jackson, J. A.; Boffey, S. J.; Valentine, P. J.; Curwen, J. O.; Musgrove, H. L.; Graham, G. A.; Hughes, G. D.; Thomas, A. P.; Stokes, E. S. E.; Curry, B.; Richmond, G. H. P.; Wadsworth, P. F.; Bigley, A. L.; Hennequin, L. F. ZD6474 inhibits vascular endothelial growth factor signaling, angiogenesis, and tumor growth following oral administration. *Cancer Res.* **2002**, *62*, 4645–4655.
- (10) Bold, G.; Altmann, K.-H.; Frei, J.; Lang, M.; Manley, P. W.; Traxler, P.; Wietfeld, B.; Bruegggen, J.; Buchdunger, E.; Cozens, R.; Ferrari, S.; Furet, P.; Hofmann, F.; Martiny-Baron, G.; Mestan, J.; Roesel, J.; Sills, M.; Stover, D.; Acemoglu, F.; Boss, E.; Emmenegger, R.; Laesser, L.; Masso, E.; Roth, R.; Schlachter, C.; Vetterli, W.; Wyss, D.; Wood, J. M. New anilinothalazines as potent and orally well absorbed inhibitors of the VEGF receptor tyrosine kinases useful as antagonists of tumor-driven angiogenesis. *J. Med. Chem.* **2000**, *43*, 2310–2323.
- (11) Wood, J. M.; Bold, G.; Buchdunger, E.; Cozens, R.; Ferrari, S.; Frei, J.; Hofmann, F.; Mestan, J.; Mett, H.; O'Reilly, T.; Persohn, E.; Rosel, J.; Schnell, C.; Stover, D.; Theuer, A.; Towbin, H.; Wenger, F.; Woods-Cook, K.; Menrad, A.; Siemeister, G.; Schirmer, M.; Thierauch, K.-H.; Schneider, M. R.; Dreves, J.; Martiny-Baron, G.; Totzke, F.; Marme, D. PTK787/ZK 222584, a novel and potent inhibitor of vascular endothelial growth factor receptor tyrosine kinases, impairs vascular endothelial growth factor-induced responses and tumor growth after oral administration. *Cancer Res.* **2000**, *60*, 2178–2189.
- (12) Joachim, J.; Hofmann, I.; Hugenschmidt, H.; Wittig, C.; Madjar, H.; Muller, M.; Wood, J.; Martiny-Baron, G.; Unger, C.; Marme, D. Effects of PTK787/ZK 222584, a specific inhibitor of vascular endothelial growth factor receptor tyrosine kinases, on primary tumor, metastasis, vessel density, and blood flow in a murine renal cell carcinoma model. *Cancer Res.* **2000**, *60*, 4819–4824.
- (13) Mendel, D. B.; Laird, A. D.; Smolich, B. D.; Blake, R. A.; Liang, C.; Hannah, A. L.; Shaheen, R. M.; Ellis, L. M.; Weitman, S.; Shawver, L. K.; Cherrington, J. M. Development of SU5416, a selective small molecule inhibitor of VEGF receptor tyrosine kinase activity, as an anti-angiogenesis agent. *Anti-Cancer Drug Des.* **2000**, *15*, 29–41.

- (14) Levin, I. J.; Turos, E.; Weinreb, S. M. An alternative procedure for the aluminium-mediated conversion of esters to amides. *Synth. Commun.* **1982**, *12*, 989–993.
- (15) PK_a determinations were carried out in parallel by potentiometric titration in water-KCl (0.15 M) with 1,4-dioxan as cosolvent.
- (16) Ertl, P.; Rohde, B.; Selzer, P. Fast Calculation of Molecular Polar Surface Area as a Sum of Fragment-Based Contributions and Its Application to the Prediction of Drug Transport Properties. *J. Med. Chem.* **2000**, *43*, 3714–3717.
- (17) Hart, I. R.; Fidler, I. J. Role of organ selectivity in the determination of metastatic patterns of B16 melanoma. *Cancer Res.* **1980**, *40*, 2281–2287.
- (18) SU5416 is not orally bioavailable and must be administered either by intraperitoneal or intravenous injection. Consequently, the compound was administered in the implant model by once-daily intraperitoneal injection. The compound was not evaluated in the mouse melanoma model.
- (19) Wood, J. M.; Schnell, C. R.; Brecht, K.; Walker, M.; Grossenbacher, R.; Fuerst, P.; Bold, G.; Ferrari, S.; Manley, P. W. Correlation between inhibition of bFGF-induced angiogenesis in an in vivo growth factor implant model and inhibition of tumor growth in tumors exhibiting different upregulation of bFGF for a series of selective VEGF receptor kinase inhibitors. *Proc. Am. Assoc. Cancer Res.* **2001**, *41*, 3127.
- (20) Manley, P. W.; Blum, W.; Bold, G.; Bruggen, J.; Hofmann, F.; Martiny-Baron, G.; Wood, J. M. NVP-AAD777/ZK202664, a selective VEGF receptor kinase inhibitor, which inhibits both VEGF- and bFGF-induced angiogenesis. *Proc. Am. Assoc. Cancer Res.* **2001**, *41*, 4470.
- (21) Potgens, A. J.; van Altena, M. C.; Lubsen, N. H.; Ruiter, D. J.; de Waal, R. M. Analysis of the tumor vasculature and metastatic behavior of xenografts of human melanoma cell lines transfected with vascular permeability factor. *Am. J. Pathol.* **1996**, *148*, 1203–1217.
- (22) Graeven, U.; Rodeck, U.; Karpinski, S.; Jost, M.; Philippou, S.; Schmiegell, W. Modulation of angiogenesis and tumorigenicity of human melanocytic cells by vascular endothelial growth factor and basic fibroblast growth factor. *Cancer Res.* **2001**, *61*, 7282–7290.

JM020899Q